USGS
science for a changing world

Geologic Map of the Big Delta B-1 Quadrangle, East-Central Alaska

By Warren C. Day, J. Michael O'Neill, John N. Aleinikoff, Gregory N. Green, Richard W. Saltus, and Larry P. Gough

Prepared in cooperation with the
Alaska Department of Natural Resources, Division of Mining, Land, and Water

Pamphlet to accompany
Scientific Investigations Map 2975

U.S. Department of the Interior
U.S. Geological Survey

U.S. Department of the Interior
DIRK KEMPTHORNE, Secretary

U.S. Geological Survey
Mark D. Myers, Director

U.S. Geological Survey, Reston, Virginia: 2007

For product and ordering information:
World Wide Web: http://www.usgs.gov/pubprod
Telephone: 1-888-ASK-USGS

For more information on the USGS—the Federal source for science about the Earth, its natural and living resources, natural hazards, and the environment:
World Wide Web: http://www.usgs.gov
Telephone: 1-888-ASK-USGS

Suggested citation:
Day, W.C., O'Neill, J.M., Aleinikoff, J.N., Green, G.N., Saltus, R.W., and Gough, L.P., 2007, Geologic map of the Big Delta B-1 quadrangle, east-central Alaska: U.S. Geological Survey Scientific Investigations Map 2975, 23-p. pamphlet, 1 plate, scale 1:63,360.

ISBN 978-1-4113-1875-5

Contents

Figures

Tables

Conversion Factors

To convert	Multiply by	To obtain
meter (m)	3.281	foot (ft)
kilometer (km)	0.6214	mile (mi)
square kilometer (km^2)	0.3861	square mile (mi^2)

Geologic Setting

Overview

The Big Delta B-1 quadrangle, east-central Alaska, lies within the Yukon-Tanana Upland and is underlain predominantly by Paleozoic and Cretaceous crystalline bedrock (fig. 1). Paleozoic units include amphibolite-facies biotite±sillimanite gneiss (Pzg and Pzgn), quartzite interlayered with metapelite (Pzq), and amphibolite gneiss (Pzam). The protoliths were continentally derived siliciclastic sediments layered with mafic volcanic rocks. These supracrustal rocks were intruded during the Devonian by plutonic rocks of felsic to intermediate composition (Dag and Dog), which, as a result of regional Mesozoic metamorphism and tectonism, are now augen gneiss and biotite orthogneiss, respectively. After assembly of the Paleozoic units during the Mesozoic deformation, the region was invaded during the Late Cretaceous by granodioritic to granitic batholiths as a response to arc plutonism along the continental margin of the North american craton. A northeast-trending structural corridor, described herein as the Black Mountain tectonic zone, both controlled the emplacement of some of the Cretaceous intrusive rocks and gold deposits and prospects, and formed a deep-seated crustal conduit along which a subsequent rhyolite flow-dome complex erupted during the Paleocene. Tertiary uplift and erosion resulted in the development of extensive erosional pediments. Quaternary alpine glaciation carved beautiful broad valleys in the eastern part of the quadrangle, leaving behind terminal moraines in the headwater region of the Eisenmenger Fork drainage. Continual deformation along the Black Mountain tectonic zone has offset Tertiary terraces, as well as Quaternary fluvial and alluvial deposits, indicating that the area has a long, complex, and ongoing tectonic history.

Paleozoic Units

The oldest units in the map area are schists and gneisses of pre-Middle Devonian age. The protolith rocks for the schist units were pelite intermixed with sandstone (Pzq), graywacke (Pzg), aluminous quartzofeldspathic epiclastic sediments (Pzgn), and basaltic flows or volcaniclastic sediments (Pzam). The depositional age of the protoliths is poorly constrained, but Aleinikoff and others (1986) dated a zircon fraction from unit Pzg of Late Devonian age (≈383 Ma), which they interpreted to be from a felsic volcaniclastic unit within the biotite schist deposited contemporaneously within the protolith sediment. Dusel-Bacon and others (2001) reported a Late Devonian crystallization age (361±3 Ma) for the protolith of the amphibolite gneiss intersected in drill core through the augen gneiss near the Brink intrusion. The supracrustal rocks were invaded by sills of trondhjemite and granodiorite. One such granodioritic horizon, or neosome, within unit Pzgn yields a crystallization age of 351±3 Ma (sample 12, table 1). Where observed, the zircons from these and similar units (Dusel-Bacon and others, 2006) have Proterozoic to Early Proterozoic cores, indicating a continental source for the sediments.

Two plutonic rock types intruded the pre-Late Devonian metasedimentary rocks—the protoliths for the augen gneiss (Dag) and the biotite orthogneiss (Dog). The augen gneiss, which is well exposed in the Central Creek watershed, forms a regionally extensive body whose protolith is interpreted to have been a granodiorite intrusion (Dusel-Bacon and Aleinikoff, 1985). Rafts of biotite schist (Pzgn) and amphibolite gneiss (Pzam) mapped within the Middle to Late Devonian augen gneiss, like those analyzed by Dusel-Bacon and others (2001), probably represent country rock entrained during the Late Devonian plutonism. Both the metamorphosed country rocks and the Devonian intrusive units were subsequently strongly deformed during regional ductile Mesozoic metamorphism and tectonism. Several mafic gneiss bodies (unit Pzmg of Day and others, 2003) form klippen on top of the augen gneiss in the Big Delta B-2 quadrangle to the west.

SHRIMP U-Pb zircon data indicate a Middle to Late Devonian igneous crystallization age for the augen gneiss (≈360–388 Ma, allowing for analytical uncertainties; Dusel-Bacon and Aleinikoff, 1985; Day and others, 2003). The augen gneiss ages overlap the crystallization age for the amphibolite gneiss (Pzam), indicating coeval, bimodal magmatism for the protoliths of units Dag and Pzam (Dusel-Bacon and others, 2006).

The other unit intruding the pre-Late Devonian supracrustal rocks is the biotite orthogneiss (Dog), whose composition includes tonalite, trondhjemite, and granodiorite. The unit forms sills and massive intrusions within the biotite schists. The few reliable crystallization ages available indicate that the unit is Devonian (sample 12, table 1; Day and others 2003), with an age range that overlaps the presumed crystallization age of the protolith of the augen gneiss (Dag). All of the zircon cores are xenocrystic and have Proterozoic to Devonian ages, indicating that the protolith melts were sourced from continental crustal material.

Mesozoic Units

Regionally, across the Yukon-Tanana Upland, peak metamorphism and deformation in the Fortymile assemblage in the eastern part of the upland of Alaska terminated in the Jurassic by about 196±4 Ma as noted by the intrusion of nonfoliated leucogranite (Day and others, 2002). However, in the Lake George assemblage (of which rocks of the study area are a part), metamorphism and ductile deformation peaked at about 117±3 Ma as recorded by metamorphic overgrowths of zircon in mylonite zones (sample 11, table 1; Day and others, 2003). The Brink intrusion, which crystallized at about 113 Ma (sample 10, table 1), is the oldest post-kinematic pluton in the map area. This follows the observations of Foster (1992), who noted that plutonism in the eastern part of the Yukon-

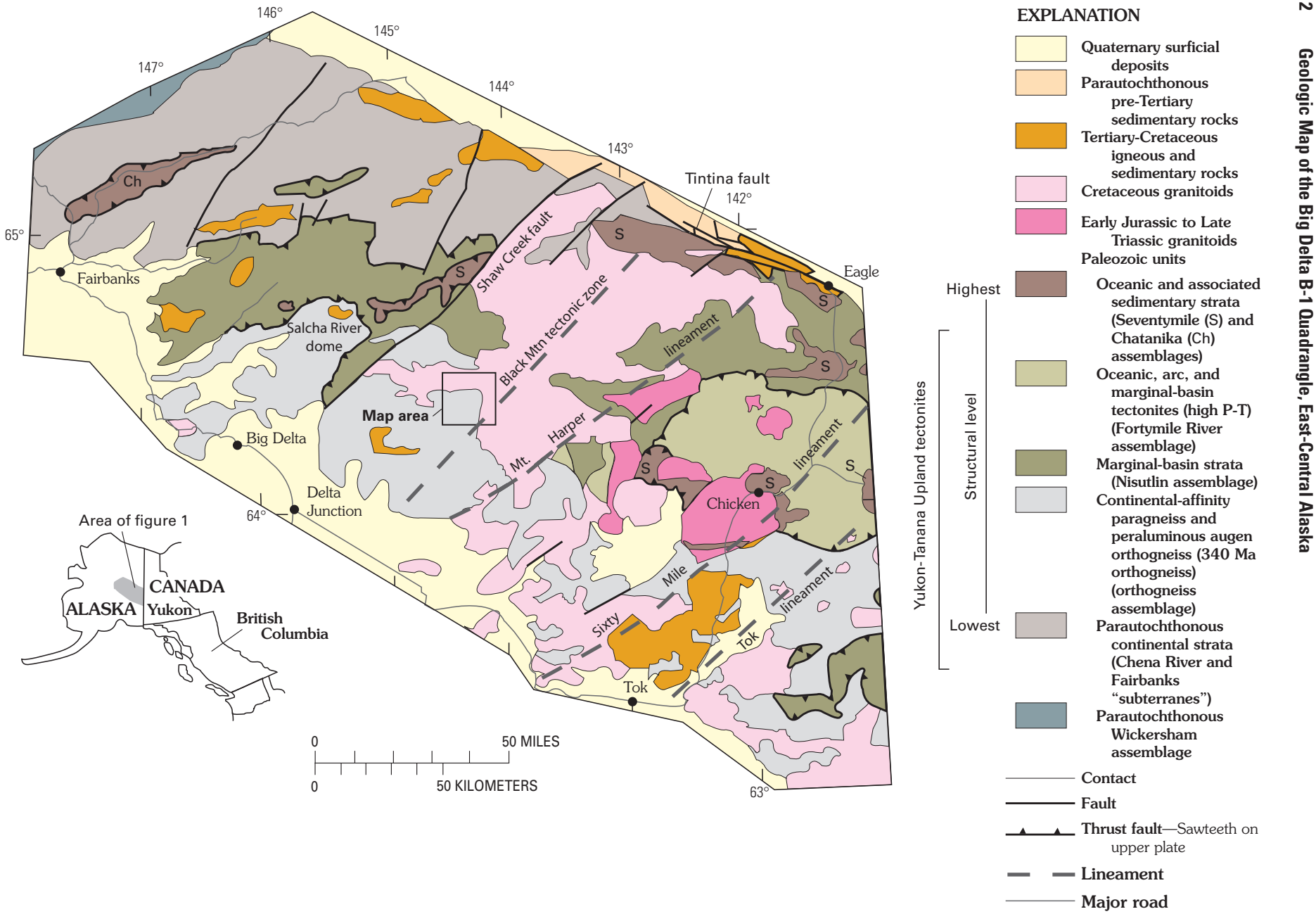

Figure 1. Tectonic assemblage of the Yukon-Tanana Upland of east-central Alaska, showing approximate outline of map area. Modified from Hansen and Dusel-Bacon (1998).

Table 1. New U-Pb SHRIMP ages for samples from the Big Delta B-1 quadrangle, east-central Alaska.

[All samples were analyzed using the USGS/Stanford sensitive high resolution ion microprobe (SHRIMP-RG) at Stanford University. The primary oxygen beam operated at about 8 nA and excavated a pit about 25 μm in diameter and 1 μm deep. Elemental fractionation was corrected using zircon standard R33 (419 Ma, Black and others, 2004). The age of each sample was determined by calculating the weighted average of $^{206}Pb/^{238}U$ ages. Raw data were reduced and plotted by using the Squid and Isoplot/Ex programs of Ludwig (1999, 2001); age errors were calculated at the 95 percent confidence limit]

Sample No.	Field station	Latitude	Longitude	Map unit	Mineral	Core/rim	Age (Ma)	Rock type
1	04AD239	64.4955°	-144.0473°	Tr	Zircon	Core	57.2±0.6	Crystal-rich rhyolite
2	05MO126	64.2699°	-144.1196°	Kqfp	Zircon	Core	95.4±0.9	Megacrystic quartz-feldspar porphyry dike
3	05AD353	64.2659°	-144.1874°	Kqfp	Zircon	Core	99.5±0.9	Megacrystic quartz-feldspar porphyry
4	03AD107	64.3327°	-144.2175°	Kbm	Zircon	Core	107.6±1.2	Nonfoliated biotite granite within Black Mountain tectonic zone
5	05AD392	64.4698°	-144.0215°	Kdi	Zircon	Core	107.9±1.1	Nonfoliated diorite dike within Black Mountain tectonic zone
6	03AD106	64.3748°	-144.1920°	Kdi	Zircon	Core	109.0±1.1	Porphyritic diorite of Black Mountain
7	03AD056	64.3431°	-144.2449°	Kgmh	Zircon	Core	110.1±1.0	Foliated biotite granodiorite of Mount Harper batholith
8	06AD415	64.3187°	-144.0199°	Kgmh	Zircon	Core	110.5±1.1	Nonfoliated biotite granodiorite of Mount Harper batholith
9	06AD431	64.4875°	-144.3174°	Kgb	Zircon	Core	109.9±1.4	Nonfoliated hornblende-biotite granodiorite of the Goodpaster batholith
10	06MO195	64.2664°	-144.3501°	Kgbr	Zircon	Core	112.9±1.3	Biotite granodiorite of Brink intrusion
11	03AD105	64.3725°	-144.4657°	Dag	Zircon	Rim	117±3	Mylonitic augen gneiss
12	04AD217	64.4126°	-144.4292°	Pzgn	Zircon	Core	351±3	Biotite granodiorite orthogneiss (Dog) neosome within unit Pzgn

Tanana Upland was both Jurassic and Cretaceous, whereas in the western part the plutonism was Cretaceous. The Early Cretaceous Mount Harper batholith, whose western margin lies in the Big Delta B-1 quadrangle, marks the easternmost extent of the Cretaceous-only plutons within the upland. As well, the Mount Harper batholith lies within the northeast-trending regional geophysical anomaly noted by Saltus (2005) and Saltus and Day (2006), which is interpreted to be the deep crustal component of the Black Mountain tectonic zone mapped herein.

The main pulse of Cretaceous plutonism occurred during the waning stages of the regional Mesozoic dynamothermal tectonism at about 111 Ma with the emplacement of the Mount Harper batholith (Kgmh), the granite of Tibbs Creek (Kgtc), and the Goodpaster batholith, all of which are I-type biotite granodiorite to granite in composition. Intrusion of the I-type biotite and hornblende-biotite granodiorite (Kbm) and hornblende-biotite diorite (Kdi) followed closely thereafter from about 109 to 107.6 Ma. This later suite of intrusions is spatially associated with known lode vein and disseminated gold (± antimony) prospects and deposits such as the Brink, Blue Lead, Gray Lead, and Grizzly Bear mines (see table 2). To the west in the Big Delta B-2 quadrangle, the Pogo gold deposit lies adjacent to the biotite-hornblende granodiorite of the Goodpaster batholith, which extends into the Big Delta B-1 quadrangle. As described in the "Tectonic History" section, the Black Mountain tectonic zone controlled the emplacement of at least the Early Cretaceous diorite dikes (Kdi) and associated lode gold vein prospects and deposits in the Big Delta B-1 quadrangle.

A distinctive second pulse of Cretaceous intrusion is represented by quartz biotite-bearing, feldspar-megacrystic porphyry dikes and small intrusions (Kqfp). U-Pb SHRIMP ages for two samples from the unit (samples 2 and 3, table 1) yield crystallization ages of 95.4±0.9 Ma and 99.5±0.9 Ma, respectively. The nonfoliated (post-kinematic) quartz feldspar porphyry was emplaced along east-northeast-trending ductile shear zones in the southeastern part of the quadrangle. The shear zones that host the Cretaceous quartz feldspar porphyry were kinematically linked to the northeast-trending faults and shear zones assigned to the Black Mountain tectonic zone.

Cenozoic Units

Paleocene (57.2±0.6 Ma) tuffs form part of a rhyolite flow-dome complex made up of crystal-rich tuffaceous flows, rhyolite dikes, and sinter deposits in the northeastern part of the Big Delta B-1 quadrangle. Post-Paleocene erosion resulted in the sculpting of broad, open terraces in the northern part of the Big Delta B-1 quadrangle, leaving behind residual boulder and gravel deposits (Tg). The surface is best developed along the current location of the Goodpaster River and in the headwaters region of the Eisenmenger Fork. Locally, gravel deposits of unit Tg are developed upon the Goodpaster batholith. The contact is a simple, conformable contact. However, the rhyolite does occur adjacent to or overlying buried northeast-trending high-angle faults associated with the northeast-trending Black Mountain tectonic zone.

Fine-grained nonfoliated basaltic dikes locally crosscut the granitoid rocks. Although the absolute age for the basaltic dikes is unknown, they may be correlative with a 50–54 Ma bimodal dike swarm commonly observed throughout the Yukon-Tanana Upland (Newberry and others, 1996).

Weber and others (1978) noted glacial deposits in the Eisenmenger Fork region of the Big Delta B-1 quadrangle and along the Boulder Creek drainage. Our mapping has revealed that the extent of glacial deposits (Qm) is limited to moraines within the U-shaped valley of the eastern fork of Boulder Creek in the southeast corner of the quadrangle.

Quaternary surficial deposits form terrace and alluvial fan deposits of sand and silt that were shed off of the highlands of crystalline basement. Active erosion has down cut through the older Paleocene and Pleistocene(?) terrace deposits, forming unconsolidated deposits of pebbles, cobbles, and boulders along the stream banks. Locally, solifluction deposits associated with freeze-thaw areas underlain by permafrost occur in the highland regions of the map area.

Tectonic History

Four distinct tectonic events recorded in the bedrock of the Big Delta B-1 quadrangle can be correlated with major magmatic-tectonic events that affected the Yukon-Tanana Upland—Devonian arc-related plutonism (D_1), Jurassic to Early Cretaceous dynamothermal convergent tectonism (D_2), Early Cretaceous ductile-brittle deformation and plutonism within the Black Mountain tectonic zone (D_3), and Paleocene to present uplift and high-angle northeast- and northwest-trending faulting related to dextral transpression within the regional wrench zone defined by Tintina-Denali fault systems (D_4).

The earliest episode of deformation (D_1) was associated with Devonian plutonism as part of a much broader regional cycle of arc-continent collision and bimodal magmatism active from the Devonian through Mississippian (Dusel-Bacon and others, 2001; Nelson and others, 2006; Piercey and others, 2006). The remnants of the mid-Paleozoic event are preserved as the bimodal magmatic suite represented by what is now the felsic Devonian augen gneiss of Central Creek (Dag), biotite orthogneiss (Dog), and the mafic gneiss bodies entrained within as country rock to the protolith granodioritic intrusion (Dusel-Bacon and others, 2001). Unfortunately, any potential penetrative D_1 structural fabrics were obliterated by regional Mesozoic deformation.

The Mesozoic tectonic event (D_2) was an intense episode of regional amphibolite-grade metamorphism and associated deformation. Evidence for Jurassic-age deformation is well documented in the amphibolite-grade schists and gneisses of the Fortymile assemblage, east of the Mount Harper batholith in the Eagle 1:250,000-scale quadrangle (see Day and others,

Table 2. Mines and prospects information from the Alaska resource data files (ARDF) for the Big Delta B-1 quadrangle, east-central Alaska (Rombach, 1999).

Mine or prospect No.	Latitude	Longitude	ARDF record No.	Mine or prospect name	Main commodity	Other commodity	Ore minerals	Deposit type
1	64.342°	-144.449°	BD011	Central Creek	Au	Unknown	Gold	Placer gold
2	64.403°	-144.302°	BD022	Last Chance Creek	Au	Unknown	Gold	Placer gold
3	64.288°	-144.263°	BD010	Carrie Creek	Au	Ag, Bi, Cu, Hg, Mo, Pb, Sb, Sn, W, Zn.	Arsenopyrite, bismuthinite, chalcopyrite, gold, molybdenite, pyrite, pyrrhotite, scheelite, sphalerite, stibnite.	Shear zone-hosted, magmatic-hydrothermal vein.
4	64.383°	-144.263°	BD040	Tibbs Creek	Au	Mo, Pb, Sb	Gold, jamesonite, molybdenite, stibnite.	Placer gold
5	64.343°	-144.249°	BD017	Gray Lead	Au	Ag, Cu, Pb, Sb	Arsenopyrite, covellite, digenite, gold, jamesonite, pyrite, stibnite.	Shear zone-hosted, magmatic-hydrothermal vein.
6	64.397°	-144.247°	BD020	Granite Creek	Au	Ag, As, Sb	Unknown	Shear zone-hosted, magmatic-hydrothermal vein.
7	64.351°	-144.209°	BD018	Grizzly Bear	Au	Ag, Cu, Pb, Sb	Arsenopyrite, covellite, digenite, gold, jamesonite, pyrite, stibnite.	Shear zone-hosted, magmatic-hydrothermal vein.
8	64.361°	-144.195°	BD025	Michigan Lode	Au	Ag, Cu, Pb, Sb	Arsenopyrite, covellite, digenite, gold, jamesonite, pyrite, stibnite.	Shear zone-hosted, magmatic-hydrothermal vein.
9	64.370°	-144.130°	BD004	Boulder Creek	Mo	Unknown	Molybdenite	Porphyry molybdenum(?)
10	64.356°	-144.194°	BD003	Blue Lead	Au	Ag, Cu, Pb, Sb	Arsenopyrite, covellite, digenite, gold, jamesonite, pyrite, stibnite.	Shear zone-hosted, magmatic-hydrothermal vein.

2002 and references therein; Dusel-Bacon and others, 2002). However, in the Lake George assemblage exposed in the Big Delta B-1 and B-2 quadrangles, evidence of Jurassic deformation recorded in an Ar-Ar cooling age from hornblende is observed only in one outcrop (Dusel-Bacon and others, 2002) of metamorphosed Devonian dioritic orthogneiss (unit Ddg of Day and others, 2003). As well, Dusel-Bacon and others (2002) reported a Jurassic Ar-Ar metamorphic cooling age from a mafic gneiss klippe that rests upon the Devonian augen gneiss (Day and others, 2003).

The new mapping has shown that the augen gneiss of Central Creek (Dag) forms a structural plate of regional extent that overlies the biotite (± sillimanite) gneiss units in the Big Delta B-1 and B-2 quadrangles (PzPzgn and PzPzg) emplaced during the waning stages of the regional D_2 event. The resulting low-angle fault is a ≈100-m-thick ductile mylonite zone at the base of the upper plate rocks. The mesoscopic structural fabrics in the augen gneiss of the upper plate differ from those in the biotite (± sillimanite) gneisses of the lower plate. In the upper plate, the augen gneiss and entrained schist units have strong stretching lineation (L-fabric) and schistosity (S- and S-C mylonitic fabrics) that consistently indicate a west-northwest sense of tectonic transport direction. The L- and S-fabrics are folded on broad open folds. In the lower plate, the biotite±sillimanite gneiss and biotite orthogneiss have steeply dipping foliations that trend northwesterly. Locally, the early foliations and granitoid neosomes are folded about westerly plunging isoclinal folds. In the lower plate, the L-fabrics are intersection and mineral lineations. Unlike in the rocks of the upper plate, stretching lineations are rare in the lower plate rocks.

A sample of zoned zircon from the basal mylonite zone within the augen gneiss from the upper plate yielded a U-Pb age of 117±3 Ma from the outer rim of the zircon (sample 11, table 1), which presumably grew during recrystallization of the augen gneiss during ductile D_2 deformation in the mylonite zone. U-Pb zircon dates from similar mylonitic thrust faults in the Big Delta B-2 quadrangle associated with D_2 deformation yield similar ages (≈116 Ma; Day and others, 2003). Therefore, the regional D_2 deformation started some time possibly in the Jurassic, extended into the Early Cretaceous, and ceased at about 116 Ma. The D_2 tectonism and associated amphibolite-grade metamorphism ceased approximately 6 m.y. prior to the main pulse of batholith emplacement, which occurred during a fairly narrow window that ranged from 111 to about 108 Ma.

The third major tectonic event (D_3) is represented by deformation observed in the northeast-striking Black Mountain tectonic zone. The Black Mountain tectonic zone was originally recognized based on regional aeromagnetic and gravity gradients that define a deep-seated, northeast-striking crustal structure that underlies the Black Mountain area (Saltus, 2005). The geophysical data indicate that the feature extends northeastward across the Yukon-Tanana Upland for over 225 km (fig. 2). As an outgrowth of the geologic mapping for this report, O'Neill and others (2005) defined the zone as a large, northeast-trending, continuous zone at least 5 km wide of mixed intrusive lithologies, which extends across the map area (fig. 3). The zone has an inner core that is underlain largely by granodiorite and is characterized not only by numerous felsic to mafic dikes, dike swarms, and small elongate plugs, but also by locally penetrative shear zones, oblique-slip normal and strike-slip faults, aligned fracture systems, and thin, highly strained screens of Paleozoic metasedimentary and metavolcanic rocks (Pzgn). The outer part of the tectonic zone (fig. 2) is a series of northeast-trending relatively high-angle normal faults that cut all of the Cretaceous and Tertiary lithologies, as well as some unconsolidated sedimentary Quaternary deposits.

The Black Mountain tectonic zone is characterized by a northeast-trending zone of complex high-angle faulting, ductile shearing, intrusion, and associated gold and antimony mineral deposits and occurrences (fig. 4). Emplacement of the ≈113 Ma Brink intrusion (sample 10, table 1), the 107.6±1.2 Ma Black Mountain intrusion (sample 4, table 1), and the diorite dikes at 107.9±1.1 Ma (sample 5, table 1) was controlled by the tectonic zone. Newberry and others (1998) dated vein muscovite from Blue Lead mine, about 1.6 km northwest of Black Mountain 105.4±0.5 Ma using the Ar-Ar technique. The Ar-Ar technique records the date for cooling of the gold mineralizing system. The time window for plutonism and associated gold mineralization is similar to that seen at the Pogo gold deposit and in gold-bearing granitoid dikes (Kgcd) to the west in the adjacent Big Delta B-2 quadrangle (see Day and others, 2003 and references therein).

Motion along the Black Mountain tectonic zone initiated during the Late Cretaceous and extended at least through the Paleocene. As discussed above, the tectonic zone controlled the emplacement of diorite dikes at about 109 Ma. The Late Cretaceous (100–95 Ma) megacrystic quartz-feldspar porphyry (Kqfp), exposed on the southeast corner of the map area, intruded along east-northeast-trending ductile shear zones associated with the tectonic zone. The quartz-feldspar porphyry dikes themselves are nonfoliated, indicating that ductile deformation along the shear zones ceased by about 100 Ma. The Paleocene rhyolite tuffs exposed in the northeast corner of the map area rest upon the Goodpaster batholith just west of the tectonic zone. The Black Mountain tectonic zone formed the conduit from which the tuffs erupted at about 57 Ma.

The fourth period of deformation (D_4) was marked by episodic regional uplift and high-angle faulting. The uplift had to have started after the Paleocene volcanism inasmuch as Tertiary gravel deposits (Tg) overlie the 57 Ma rhyolite tuffs in the northeastern part of the quadrangle. Fault scarps are also preserved in the Quaternary surficial deposits. The map area is crosscut by both northeast- and northwest-striking high-angle brittle faults. The major northeast-striking faults show left-lateral sense of offset. The northwest-striking faults have fewer piercing points; but, where present, they indicate a right-lateral sense of offset.

Acknowledgments

This research was funded by the U.S. Geological Survey Mineral Resource Program. The authors benefited greatly from discussions about the complexity of the regional geology and the history of geologic research with Cynthia Dusel-Bacon (USGS), Jack DiMarchi (Teck Cominco, Limited), Richard Goldfarb (USGS), Rainer Newberry (University of Alaska-Fairbanks), Jim Vohden (Alaska Department of Natural Resources, Division of Mining, Land, and Water), and Melanie Werdon (Alaska Department of Natural Resources, Division of Geological and Geophysical Surveys). Logistical support was generously provided by the Alaska Department of Natural Resources, Division of Mining, Land, and Water. Our work was improved by thoughtful and detailed reviews by Donald Sweetkind (USGS) and Melanie Werdon. Alex Donatich (USGS) provided technical guidance during preparation and production of this map. All of the mistakes, however, are wholly the responsibility of the primary author.

Mapping Credits

The geologic mapping was conducted during several one to two week-long field seasons during 2003–2006 by W.C. Day and J.M. O'Neill. The location of buried structures and geologic contacts was greatly aided by the detailed geophysical data published by Burns and others (2006) and the regional aeromagnetic data provided by R.W. Saltus, based in large part on the State-wide aeromagnetic data compilation of Saltus and Simmons (1997). Previous reconnaissance geologic mapping by Weber and others (1975) helped guide our mapping effort.

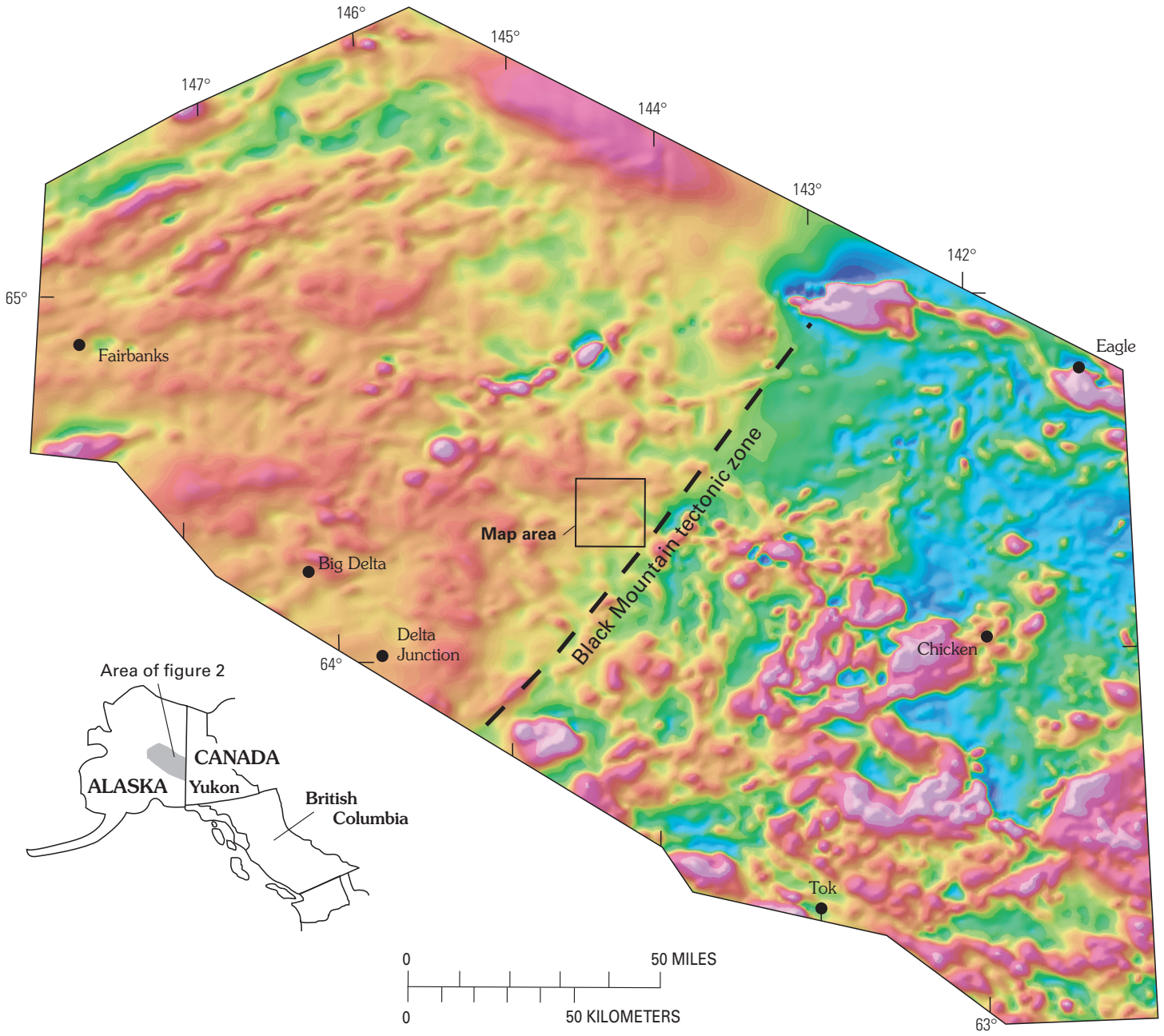

Figure 2. Regional aeromagnetics of the Yukon-Tanana Upland of east-central Alaska. Modified from Saltus and Simmons (1997).

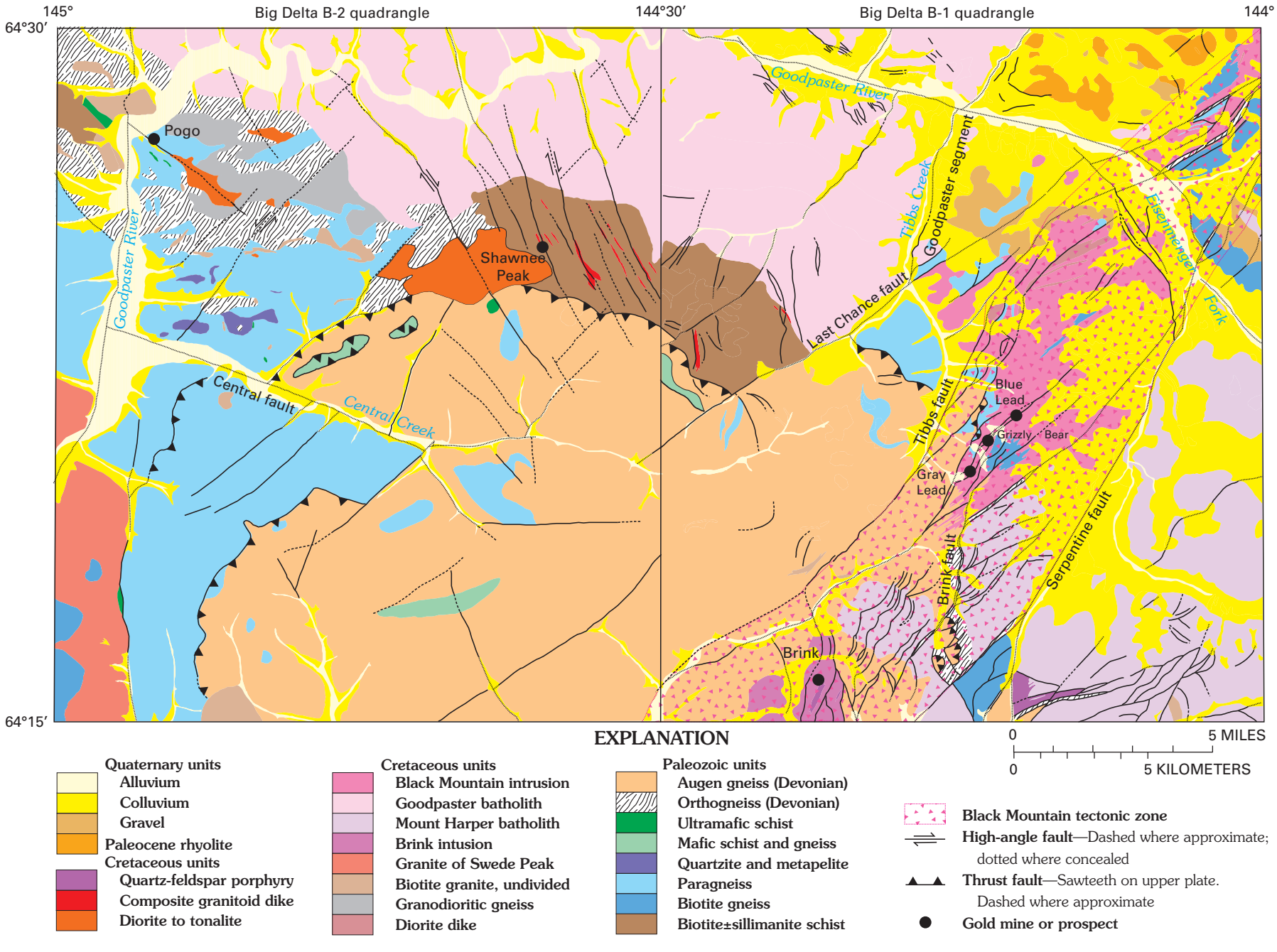

Figure 3. Simplified geology of the Big Delta B-1 and B-2 quadrangles, east-central Alaska, showing the location of gold mines and prospects and the surficial expression of the Black Mountain tectonic zone.

Figure 4. Brecciated stibnite-bearing quartz vein material from Grizzly Bear mine dump (field station 03AD062; lat 64.3569° N., long 144.1929°W.).

DESCRIPTION OF MAP UNITS

QUATERNARY AND TERTIARY SURFICIAL DEPOSITS

Qfp **Flood-plain deposits (Holocene)**—Silt, sand, and gravel in flood plains of primary rivers and in some smaller periglacial channels of smaller tributaries; includes thick boulder gravel deposits and glacial outwash along Boulder Creek in east-central part of map area. Maximum thickness unknown

Qaf **Alluvial and fluvial deposits (Holocene)**—Clay, silt, sand, and pebble to cobble gravel deposited in narrow stream channels and on broad alluvial slopes at base of low hills and mountain fronts and on steeper mountain flanks; locally includes minor colluvium (Qc). Maximum thickness unknown

Qc **Colluvium (Holocene)**—Residual deposits of clay, silt, sand, and angular pebbles and cobbles that mantle shallow-dipping slopes; most common in weakly dissected terrane in eastern part of map area. Thickness uncertain, but probably less than 1 m

Qfy **Young alluvial fan deposits (Holocene)**—Poorly sorted silty sand and gravel that form small alluvial fans along margins of all major stream drainages. Maximum thickness unknown

Qls **Landslide deposits (Holocene)**—Angular fragments of bedrock mixed with soil, or heterogeneous mixtures of boulders and finer grained material derived from adjacent steep hill slopes; characterized by irregular-shaped, hummocky topography and numerous closed depressions. Maximum thickness unknown

Qsl **Solifluction deposits (Holocene)**—Unsorted, water-saturated colluvial material restricted to unglaciated, higher mountain peaks mostly in western part of map area; characterized by numerous elongate terraced or flattish areas that step down into adjacent active drainage. Maximum thickness less than 4 m

Qd **Debris flow deposits (Holocene)**—Coarse, unconsolidated deposits of locally derived, angular pebbles, cobbles, and boulders associated with fine-grained matrix of sand and silt; confined to steep alpine gulches in west-central part of map area

Qt **Terrace deposits (Holocene and Pleistocene?)**—Fluvial sand and pebble-size gravel deposits restricted to Goodpaster River and its main tributary, the Eisenmenger Fork, in northern part of map area; interfingers with older alluvial fan deposits (Qfo). Maximum thickness unknown

Qfo **Old alluvial fan deposits (Holocene and Pleistocene?)**—Poorly sorted silty sand and gravel deposited in inactive, generally large alluvial fans along the Goodpaster River and its tributaries in eastern part of map area; interfingers with terrace deposits (Qt). Maximum thickness unknown

Qm **Glacial moraine deposits (Holocene and Pleistocene?)**—Poorly sorted, unconsolidated deposits of silt, sand, gravel, and boulders in small glacial cirques in southeastern part of map area and in adjacent, upper reaches of Boulder Creek. Maximum thickness unknown

TERTIARY SEDIMENTARY ROCKS

Tg **Gravel-rich terrace deposits (post-Paleocene)**—Residual boulder and gravel deposits with lesser amounts of clay, sand, and silt (fig. 5) deposited on flat to gently sloping undissected surfaces throughout northeastern extent of map area at elevations between 300 and 600 m above adjacent drainages. These deposits, and the surface upon which they lie, overlie Paleocene welded tuffs (Tr) in northeastern part of map area. These residual deposits are interpreted to preserve beneath their cover a middle Tertiary erosion surface developed prior to major incision of the Goodpaster River and its main tributaries

TERTIARY IGNEOUS ROCKS

Tb **Basalt dikes (Eocene?)**—Dark-gray to black, nonfoliated basalt dikes containing small, randomly oriented plagioclase phenocrysts set in devitrified aphanitic groundmass. Age uncertain, but may be correlative with a 50–54 Ma suite of bimodal volcanic rocks; basaltic dike swarms are commonly associated with these rocks throughout this part of the Yukon-Tanana Upland (Newberry and others, 1998)

Trd **Rhyolite dikes (Tertiary)**—Light-gray, nonfoliated rhyolite dikes containing as much as 10 percent feldspar phenocrysts set in an aphanitic groundmass. Dikes are thin, approximately 1–3 m wide, and cut Cretaceous intrusive units. Unit crosscuts both Cretaceous intrusive and Tertiary rhyolitic volcanic rocks. Absolute age uncertain, but presumed to be either part of the Tertiary volcanism expressed in northeastern part of quadrangle (Tr) or part of 50–54 Ma suite of bimodal volcanic rocks associated with unit Tb

Tr **Rhyolite (Paleocene)**—Dark-gray to white, crystal-rich biotite-hornblende rhyolitic welded tuff. Phenocrysts, including quartz, sanidine, biotite, and hornblende, make up as much as 20–25 percent of rock. Local silicic and argillic alteration (fig. 6). Contains vent-facies devitrified crystal-rich rhyolite vitrophyre (fig. 7). Tectonism of unit limited to minimal high-angle faulting and associated fracturing. Part of rhyolite flow-dome complex in northeastern part of quadrangle that straddles and potentially overlies the Black Mountain tectonic zone exposed immediately east of volcanic complex. A U-Pb SHRIMP analysis determined from zircon in samples collected during this study yielded a Paleocene age of 57.2±0.6 Ma (sample 1, table 1). Rhyolitic rocks collected directly north of map area by Foster and others (1979) yielded a K-Ar age of 61.6±2 Ma

CRETACEOUS IGNEOUS ROCKS

Exposed Cretaceous igneous rocks range from leucogranite to diorite. Granite and granodiorite are the most abundant bedrock types in area and make up five major intrusions; from west to east, these rocks form the Goodpaster batholith, biotite granite of Tibbs Creek, granodiorite of the Brink intrusion, Black Mountain intrusion, and Mount Harper batholith. Associated with these rocks, but restricted to major northeast-trending shear zones in central and southeastern parts of map area, are Cretaceous dikes and plugs of diorite, quartz-feldspar porphyry, leucogranite, and pegmatite, and quartz veins. Diorite dikes have textures that suggest a subvolcanic setting for their emplacement in the root zone of a Cretaceous volcano-plutonic complex. Relative age relations between the larger intrusive bodies are not everywhere clear. New radiometric ages are reported herein for most of the igneous rock

Kpeg **Pegmatitic dikes (Late Cretaceous?)**—Nonfoliated, light-pink to light-gray pegmatite dikes of granitic composition; major minerals are quartz, plagioclase, alkali feldspar, biotite, and muscovite. Pegmatitic dikes texturally and compositionally grade into quartz veins. Age uncertain, but assumed to have been emplaced during the latest part of the regional Cretaceous intrusive event

Kg **Biotite granite (Late Cretaceous?)**—Light-gray, equigranular, medium-grained biotite granite. Intrudes granite of Mount Harper batholith (Kgmh) in southeastern part of quadrangle. May be correlative with quartz-feldspar porphyry (Kqfp) intrusive

Kqfp **Quartz-feldspar porphyry (Late Cretaceous)**—Quartz-feldspar porphyry dikes and small intrusions. Unit characterized by megacrysts and glomeroporphyritic phenocryst clusters of plagioclase (as much as 4 cm diameter), rounded quartz (as much as 2 cm diameter), and minor biotite set in a medium-gray, fine-grained groundmass of rhyolitic composition containing individual phenocrysts of quartz, feldspar, biotite, and opaque minerals. Forms dikes and small intrusions in southern part of quadrangle. Locally cut by quartz veins (fig. 8). U-Pb SHRIMP ages for two samples from unit (samples 2 and 3, table 1) yield crystallization ages of 95.4±0.9 Ma and 99.5±0.9 Ma, respectively. Unit interpreted to be emplaced adjacent to and along east-northeast-trending splay of Black Mountain tectonic zone in southeastern part of map area during the Late Cretaceous

Kgcd **Granitoid dikes and plugs (Early Cretaceous)**—Composite granitoid dikes restricted to northwestern part of map area, west of Last Chance fault; highly variable compositions include light-gray, fine-grained, equigranular, nonfoliated biotite granodiorite, coarse-grained leucogranite, and biotite-quartz-alkali-feldspar pegmatite that intrude metamorphosed Paleozoic rocks (PzPgn). Late-stage quartz veins cut earlier dikes. Plagioclase phenocrysts exhibit characteristic strong compositional zonation. Potassium- and silica-rich gossans commonly developed in adjacent country rock. Zones of anomalous gold and sulfide-mineral (pyrite, arsenopyrite, stibnite) concentrations occur in both quartz veins and pegmatitic zones in country rock near dike margins in adjacent Big Delta B-2 quadrangle (Day and others, 2003). U-Pb SHRIMP dating of zircon overgrowths on Precambrian to Paleozoic xenocrystic cores indicates a crystallization age of 106±3 Ma from this unit in Big Delta B-2 quadrangle (sample 01AD-257 of Day and others, 2003)

Kdi **Diorite dikes (Early Cretaceous)**—Dark-gray to dark-green, nonfoliated biotite-hornblende diorite dikes. Unit contains distinctive medium-grained, subhedral hornblende-biotite and plagioclase phenocrysts and glomerocrysts set in a fine-grained dioritic matrix; interpreted to be emplaced as subvolcanic dikes and small intrusions. U-Pb SHRIMP dating of zircon yields a primary crystallization age of between 107.9±1.1 Ma and 109.0±1.1 Ma (samples 5 and 6, respectively, table 1). Emplaced as northeast-trending dikes within and along Black Mountain tectonic zone; displays aphanitic, chilled margin where it cuts unit Kbm

Kbm **Black Mountain intrusion (Early Cretaceous)**—Composite intrusion predominantly made up of biotite granite and biotite-hornblende granodiorite, with lesser amounts of coeval hornblende-biotite diorite. Granitic to granodioritic phases are medium gray, nonfoliated, medium grained, and equigranular to porphyritic (fig. 9) with distinctive lath-shaped clots of biotite, hornblende, and plagioclase set in a medium- to fine-grained matrix. Mafic phase of composite intrusion is made up of dark-gray to dark-green,

nonfoliated, porphyritic, hornblende-biotite diorite equivalent in composition, texture, and age to unit Kdi. U-Pb SHRIMP date from zircon yields an age of 107.6±1.2 Ma for a biotite granodiorite from the spine of Black Mountain (sample 4, table 1). Diorite locally observed to cut the granodiorite phase of intrusive complex. Where diorite occurs in large enough areas it is mapped as unit Kdi. Nonfoliated (post-ductile deformation) diorite dike (Kdi) dated at 107.9±1.1 Ma (sample 5, table 1) in Black Mountain tectonic zone north of Eisenmenger Fork of Goodpaster River. Porphyritic diorite dike (Kdi) from northern extent of Black Mountain, within the intrusion proper, yields a U-Pb SHRIMP date on zircon of 109.0±1.1 Ma (sample 6, table 1). U-Pb ages of granodiorite phase and dioritic phases overlap within analytical error; where observed, unit Kdi intrudes unit Kbm. Both units Kdi and Kbm were emplaced within Black Mountain tectonic zone

Goodpaster batholith (Early Cretaceous)—Composite batholith composed predominantly of nonfoliated, coarse-grained, equigranular hornblende-biotite granodiorite (Kgb) with volumetrically minor late-phase intrusions of leucogranite and pegmatite; a foliated border phase bounds the batholith along its southern margin in map area (Kgbf). New U-Pb SHRIMP age from euhedral zircons from the nonfoliated post-kinematic core (Kgb) of batholith (sample 9, table 1) yields an age of crystallization of 109.9±1.4 Ma. Unit is temporally correlative with the Mount Harper batholith (Kgmh).

The Pogo gold deposit, located within Big Delta B-2 quadrangle to the west, is a blind mineral deposit hosted in Paleozoic gneisses adjacent to southern margin of Goodpaster batholith (Day and others, 2003; Werdon and others, 2004). Dilworth and others (2002) reported an age range of 107–109 Ma (U-Pb zircon) for late-kinematic granitic plutonism, and as young as ≈104 Ma for post-kinematic plutonism within the area of the Pogo gold deposit. Similarly, Smith and others (1999), Smith (2000), and Selby and others (2002) reported a U-Pb date on monazite for granitic dikes at Pogo of 107 Ma and a Re-Os age on molybdenite vein samples of 104.2 Ma. Other $^{40}Ar/^{39}Ar$ age dates reported by Selby and others (2002) in nonmineralized rocks at Pogo include biotite in diorite at 94.5 Ma and a biotite age from a diabase dike cutting a gold-bearing ore zone at 92.7 Ma

Kgb **Main intrusive phase**—Equigranular, nonfoliated, coarse-grained hornblende-biotite granodiorite. Locally weathers to distinctive ochre-colored grus. Unit forms relatively low-lying rounded hills along center of Goodpaster River watershed

Kgbf **Early intrusive phase**—Medium-grained, hypidiomorphic, equigranular, moderately foliated biotite ± hornblende granodiorite along southern margin of Goodpaster batholith. Foliation parallels east-trending trace of southern margin of batholith; interpreted to be flow foliation related to emplacement of batholith. Unit distinguished from adjacent biotite granite of Tibbs Creek (Kgtc) by local presence of hornblende, a foliated fabric, and only minor sericitic and iron oxide alteration

Kgmh **Granitic rocks of Mount Harper batholith (Early Cetaceous)**—Predominantly medium-grained, equigranular, light-gray to light-pink, massive, nonfoliated biotite granodiorite to granite (figs. 10 and 11) with local enclaves of hornblende-biotite diorite. Locally, a weak to moderate foliation is preserved on west margin of batholith, which is interpreted to be a result of shearing along margin during emplacement of intrusion. Mount Harper batholith was named for exposures of granodiorite that underlies the Mount Harper area in southwestern part of Eagle quadrangle, directly east of map area. The batholith was named and originally mapped by Weber and others (1978). U-Pb SHRIMP analyses of zircon from weakly to moderately foliated rocks, interpreted as a border phase of Mount Harper batholith, yield an age of crystallization of 110.1±1.0 Ma (sample 7, table 1). A sample taken from nonfoliated central part of intrusion also has a primary age of crystallization at 110.5±1.1 Ma (sample 8, table 1). Dusel-Bacon and others (2002) reported an $^{40}Ar/^{39}Ar$ age on biotite from a sample taken along east margin of Mount Harper batholith 24 km east of the map area of 106.7± 0.6 Ma. Newberry and others (1998) reported an $^{40}Ar/^{39}Ar$ plateau age of 102.7±0.4 Ma on vein muscovite from a prospect pit within unit Kgmh, approximately 10 km southwest of locality of sample reported in Dusel-Bacon and others (2002)

Kgtc **Granite of Tibbs Creek (Early Cretaceous)**—Medium-grained, nonfoliated to weakly foliated, equigranular, light-gray, massive biotite granite. Unit is relatively fresh on east side of Tibbs Creek; highly altered west of Tibbs Creek near contact zone with Goodpaster batholith. Primary feldspar and biotite altered to intergrowths of iron oxide, sericite, chlorite, and needles of sillimanite. Similar sillimanite alteration seen in Paleozoic units of granodioritic bulk composition south of Goodpaster batholith to the west in Big Delta B-2 quadrangle (Day and others, 2003), recording broad regional hydrothermal alteration associated with emplacement of Goodpaster batholith. Altered areas have distinctive ochre-colored soil. Interpreted to be older than Goodpaster batholith

Kgbr **Granodiorite of Brink intrusion (Early Cretaceous)**—Light-gray to white, nonfoliated, coarse-grained biotite ± hornblende granodiorite (fig. 12). Gold mineralization associated with late-stage quartz veins within pluton. U-Pb SHRIMP crystallization age of Brink intrusion is 112.9±1.3 Ma (sample 10, table 1). As such, unit represents oldest recognized intrusive phase related to the Early Cretaceous pulse of plutonism within map area. Unit lies within core of Black Mountain tectonic zone, implying tectonic zone may have been controlling emplacement of plutonic units at least as early as about 113 Ma

PALEOZOIC AND OLDER METAMORPHIC UNITS

Dag **Augen gneiss of Central Creek (Late and Middle Devonian)**—Multiphase orthogneiss dominated by light-gray, medium- to coarse-grained, strongly foliated biotite-muscovite ± sillimanite quartzofeldspathic augen gneiss (fig. 13); lesser relatively augen-free biotite gneiss of granodioritic to granitic bulk composition. Unit is characterized by lenticular-shaped augen made up of relict alkali feldspar porphyroclasts (as much as 5 cm diameter) and porphyroblasts of quartz, feldspar, mica ± garnet mineral aggregates set in a medium-grained, foliated to granoblastic matrix of granodioritic composition. Forms regionally extensive, coherent body that extends from Big Delta B-1 quadrangle approximately 32 km westward to Sonora Creek in Big Delta B-2 quadrangle (Day and others, 2003), underlying most of headwater region for Central Creek. Anastomosing mica-rich shear bands separate zones of both equigranular matrix and augen into sigmoid-shaped zones (mesolithons). Mesolithons commonly have asymmetric tails forming oriented "fish" bounded by micaceous shear bands that display S-C mylonitic fabrics formed during ductile regional metamorphism. Contact with structurally underlying early Paleozoic metamorphic unit PzPzgn is a high-strain mylonite, with ribbon quartz and S-C mylonitic fabrics (fig. 14); tectonic transport direction consistently west-northwest vergent in map area.

Age of tectonism responsible for ductile deformation and thrust faulting unit Dag over PzPzgn inferred to be Early Cretaceous (≈114–117 Ma) based on U-Pb SHRIMP age from metamorphic overgrowth on zoned zircon collected from a basal mylonite zone exposed at saddle between Last Chance and Central Creeks (117±3 Ma; sample 11, table 1) and from similar mylonitic horizons in adjacent Big Delta B-2 quadrangle (samples 02AD339 and 01AD-213 of Day and others, 2003). Dusel-Bacon and Aleinikoff (1985) described the regional geologic context for the unit and suggested a plutonic protolith. Dusel-Bacon and others (2001) reported a Late Devonian U-Pb zircon SHRIMP age of 362±3 Ma (their sample AG-2 of euhedral zircon) from an augen gneiss sample taken north of Central Creek and west of California Creek in adjacent Big Delta B-2 quadrangle. Day and others (2003) reported a U-Pb zircon SHRIMP age of 365±4 Ma (Late Devonian) for unit (their sample AG-3, table 1). A sample from same map unit yielded a Middle Devonian age of 388±3 Ma as reported by Dusel-Bacon and others (2001; their sample AG-5). Aleinikoff and others (1981; their sample AG-5) reported K-Ar dates on muscovite of 113±4 Ma and on biotite of 110±4 Ma, reflecting post-peak metamorphic cooling during the Cretaceous. These K-Ar metamorphic cooling ages are slightly younger than the 117±3 Ma age from a metamorphic overgrowth on zircon taken from a mylonite zone within the augen gneiss (sample 11, table 1)

Dog **Biotite orthogneiss (Late and Middle Devonian)**—Predominantly light- to medium-gray, medium-grained, layered tonalitic, trondhjemitic to granodioritic orthogneiss (fig. 15);

lesser amounts of biotite schist, quartzite, and paragneiss. Unit in Big Delta B-2 quadrangle contains xenocrystic zircon cores that vary in age from ≈367 Ma to ≈1,184 Ma (Day and others, 2003; sample 02AD339, table 1). One zircon core yields a perplexing U-Pb SHRIMP age of 367±7 Ma and is rimmed by a 380±12 Ma moderately zoned (igneous) zircon overgrowth. Both Devonian ages are within error of each other and indicate a Late to Middle Devonian emplacement age of the protolith, which is equivalent to or slightly older than that of the protolith for the augen gneiss unit Dag. U-Pb SHRIMP ages on zircon rims show two populations—an older group at 114±2 Ma and a younger group at 109±2 Ma (Day and others, 2003; sample 02AD339, table 1). U-Pb SHRIMP data on zircons from unit indicate that protolith intrusion inherited zircons from a crustal source that was in part Precambrian, was emplaced during the Devonian, and was recrystallized twice during pulses of regional Cretaceous tectonism at ≈114 Ma and at ≈109 Ma

Pzam **Amphibolite gneiss (Late Devonian and older)**—Dark-green, fine- to medium-grained, strongly foliated, hornblende-biotite amphibolite gneiss interlayered with foliated, medium-grained, equigranular calc-silicate schist and, locally, quartzite. Protolith could have been mafic tuff or volcanic horizon intercalated with sediments. Unit occurs as rafts within augen gneiss (Dag) as well as in northeastern part of quadrangle within Black Mountain tectonic zone. Dusel-Bacon and others (2001) reported a Late Devonian crystallization age (361±3 Ma) for the protolith of an amphibolite gneiss horizon intersected in drill core within the augen gneiss. Assuming plutonic origin for the augen gneiss protolith, unit was probably country rock during intrusion of protolith of augen gneiss, indicating a minimum age of Late Devonian for the mafic volcanic and sedimentary protoliths

Pzq **Quartzite and metapelite (pre-Late Devonian)**—Light-gray, equigranular, muscovite-bearing feldspathic quartzite interlayered with micaceous schist (metapelite). Protoliths were immature sandstone interlayered with pelite. Age uncertain, but protolith assumed to be part of now structurally disrupted sedimentary sequence that included the protoliths for unit Pzgn

Pzgn **Biotite±sillimanite gneiss (pre-Middle Devonian)**—Medium- to dark-gray, medium-grained, foliated, equigranular, biotite-rich gneissic migmatite. Migmatite is made up of a paleosome of medium-gray, equigranular, medium- to fine-grained, quartzofeldspathic biotite±sillimanite schist invaded by a neosome of biotite trondhjemitic to granodioritic orthogneiss (fig. 16). Metamorphic mineral assemblage includes biotite, muscovite, garnet, and, locally, sillimanite. Protolith for unit was graywacke to muddy siliciclastic sediment and sandstone. Neosome is light-gray, medium-grained, foliated biotite trondhjemitic to granodioritic orthogneiss enfolded with the paleosome; foliation in orthogneiss is conformable with that in the paleosome country rock. U-Pb SHRIMP analysis on zircon from orthogneiss neosome yields a crystallization age of 351±3 Ma (sample 12, table 1) for a granodiorite horizon within the migmatitic gneiss. Unit equivalent to biotite-sillimanite gneiss (Pzgn) of Day and others (2003). Paleosome thought to represent country rock at time of intrusion of protolith for Middle to Late Devonian augen gneiss (Dag), thus making the unit pre-Middle Devonian

Pzg **Biotite gneiss (pre-Late Devonian)**—Medium-gray, medium-grained, quartzofeldspathic biotite gneiss. Inherited zircons from metavolcanic rocks interlayered within unit south of map area (unit Pzpeg of Weber and others, 1978), yet one sample yielded a Devonian $^{207}Pb/^{206}Pb$ age of approximately 383 Ma (Aleinikoff and others, 1986; sample 4017; –400 mesh fraction), representing upper age limit for deposition of the protolith

Figure 5. Gravel-rich terrace deposit made up of rounded granitic boulders, cobbles, and pebbles set in sandy matrix (Tg; field station 06AD434; lat 64.4371° N., long 144.0159° W.).

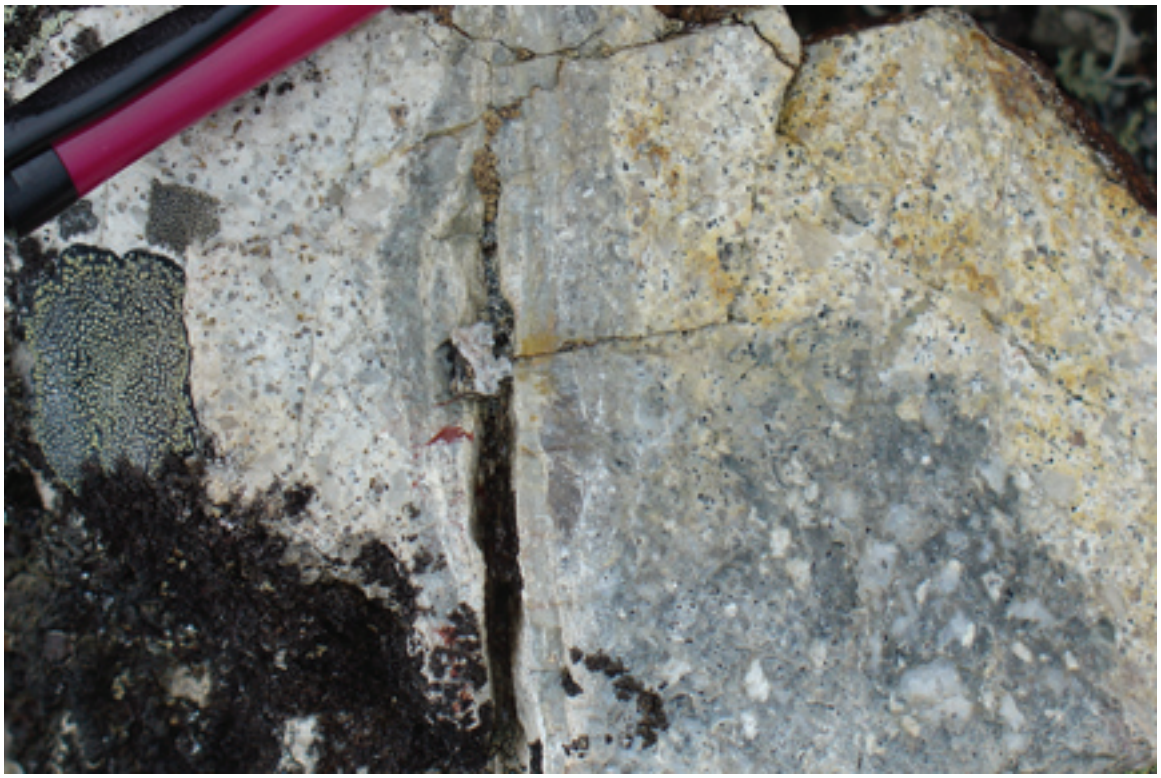

Figure 6. Localized vein of silicification within typical Paleocene crystal-rich hornblende-biotite rhyolite (Tr; field station 04AD241; lat 64.4931° N., long 144.0549° W.).

Figure 7. Black, crystal-rich rhyolitic vitrophyre phase of unit Tr, which forms a Paleocene rhyolite flow-dome complex in northeastern part of quadrangle (field station 04AD242; lat 64.4933° N., long 144.0623° W.).

Figure 8. Quartz vein cutting Late Cretaceous megacrystic quartz-feldspar porphyry (Kqfp). Specimen (sample 3, table 1) of unit Kqfp taken nearby yielded a U-Pb age of 99.5±0.9 Ma (field station 05AD353; lat 64.2659° N., long 144.1874° W.).

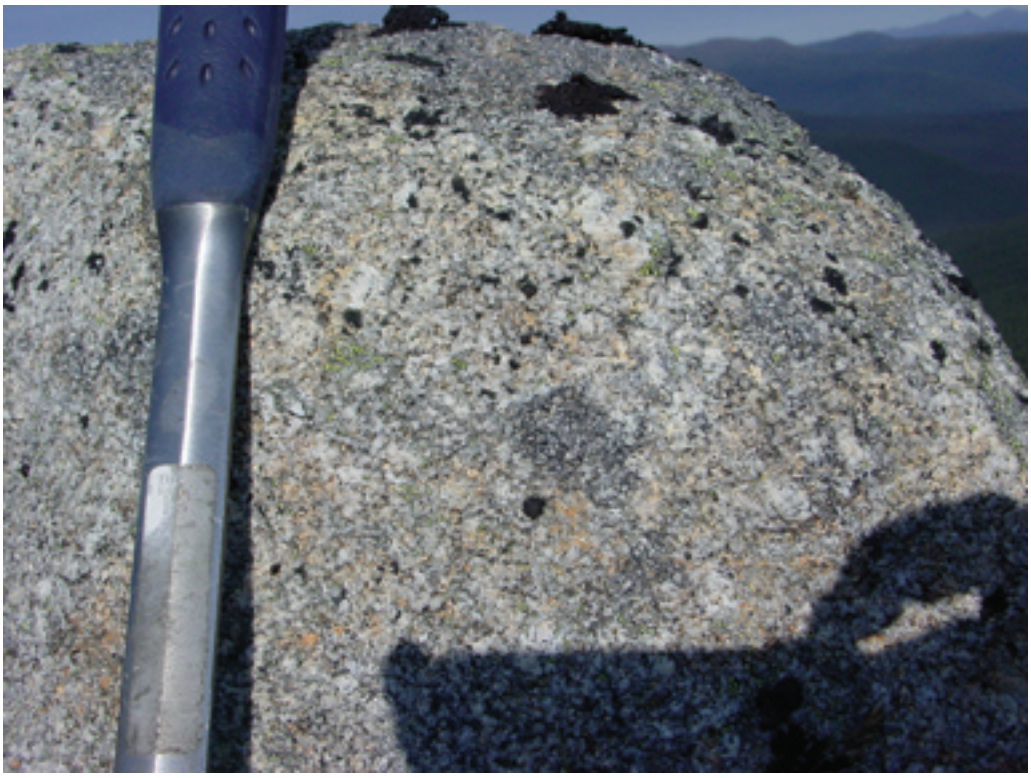

Figure 9. Nonfoliated porphyritic hornblende-biotite granodiorite phase of Early Cretaceous Black Mountain intrusion (Kbm; field station 03AD066; lat 64.3482° N., long 144.2016° W.).

Figure 10. Nonfoliated phase of Early Cretaceous Mount Harper biotite granite (Kgmh; field station 04AD232; lat 64.3569° N., long 144.0194° W.).

Figure 11. Medium-grained equigranular phase of Early Cretaceous Mount Harper batholith (Kmh; field station 05AD322; lat 64.2851° N., long 144.2304° W.).

Figure 12. Medium-grained equigranular hornblende-biotite granodioritic phase of Early Cretaceous Brink intrusion (Kgbr; field station 06AD453; lat 64.2614° N., long 144.3542° W.).

Figure 13. Typical Devonian augen gneiss (Dag). Kinematic fabrics that formed during the regional Late Cretaceous dynamothermal tectonism indicate northwest-vergent down-dip direction (to the right) of tectonic transport (field station 06AD476; lat 64.3493° N., long 144.3596° W.).

Figure 14. High-strain zone within Devonian augen gneiss (Dag) near basal zone of upper structural plate. See "Tectonic History" section for description of upper and lower structural plates. Ductile S-C mylonitic fabrics indicate sense of northwest vergence (to the right) of upper plate (field station 03AD050; lat 64.3354° N., long 144.2480° W.).

Figure 15. Foliated and lineated fabric in Devonian biotite orthogneiss (Dog; field station 05AD338; lat 64.2649° N., long 144.2421° W.).

Figure 16. Open fold of boudinaged layers of biotite-rich paragneiss and interlayered granitic stringers in Paleozoic gneiss (Pzgn) cut by Cretaceous granite dike. Regionally, unit forms lower structural plate. See "Tectonic History" section for definition of upper and lower plates that define the pre-Cretaceous structural architecture of area (field station 04AD208; lat 64.4137° N., long 144.4724° W.).

References Cited

Aleinikoff, J.N., Dusel-Bacon, Cynthia, and Foster, H.L., 1986, Geochronology of augen gneiss and related rocks, Yukon-Tanana terrane, east-central Alaska: Geological Society of America Bulletin, v. 97, p. 626–637.

Aleinikoff, J.N., Dusel-Bacon, Cynthia, Foster, H.L., and Futa, Kiyoto, 1981, Proterozoic zircon from augen gneiss, Yukon-Tanana Upland, east-central Alaska: Geology, v. 9, p. 469–473.

Black, L.P., Kamo, S.L., Allen, C.M., Davis, D.W., Aleinikoff, J.N., Valley, J.W., Mundil, R., Campbell, I.H., Korsuch, R.J., Williams, I.S., and Foudoulis, C., 2004, Improved $^{206}Pb/^{238}U$ microprobe geochronology by the monitoring of a trace-element-related matrix effect; SHRIMP, ID–TIMS, ELA–ICP–MS and oxygen isotope documentation for a series of zircon standards: Chemical Geology, v. 205, p. 115–140.

Burns, L.E., Fugro Airborne Surveys, and Stevens Exploration Management Corp., 2006, Line, grid, and vector data and plot files for the airborne geophysical survey data of parts of the East Richardson, Liscum, and Black Mountain areas, Interior Alaska: Alaska Division of Geological and Geophysical Surveys Geophysical Report 2006-5, 2 disks.

Day, W.C., Aleinikoff, J.N., and Gamble, B.M., 2002, Geochemistry and age constraints on metamorphism and deformation in the Fortymile River area, eastern Yukon-Tanana Upland, Alaska, *in* Wilson, F.H., and Galloway, J., eds., Studies by the U.S. Geological Survey in Alaska, 2000: U.S. Geological Survey Professional Paper 1662, p. 5–18.

Day, W.C., Aleinikoff, J.N., Roberts, Paul, Smith, Moira, Gamble, B.M., Henning, M.W., Gough, L.P., and Morath, L.C., 2003, Geologic map of the Big Delta B-2 quadrangle, east-central Alaska: U.S. Geological Survey Geologic Investigations Series I–2788, 1 sheet, scale 1:63,360.

Dilworth, Katherine, Ebert, Shane, Mortensen, J.K., Rombach, Cameron, and Tosdal, R.M., 2002, Reduced granites and gold veins in the Pogo area, east-central Alaska: Geological Society of America Abstracts with Programs, v. 34, no. 6, p. 114.

Dusel-Bacon, Cynthia, and Aleinikoff, J.N., 1985, Petrology and tectonic significance of augen gneiss from a belt of Mississippian granitoids in the Yukon-Tanana terrane, east-central Alaska: Geological Society of America Bulletin, v. 96, p. 411–425.

Dusel-Bacon, Cynthia, Hopkins, M.J., Mortensen, J.K., Dashevsky, S.S., Bresler, J.R., and Day, W.C., 2006, Paleozoic tectonic and metallogenic evolution of the pericratonic rocks of east-central Alaska and adjacent Yukon, *in* Colpron, Maurice, and Nelson, JoAnne, eds., Paleozoic evolution and metallogeny of pericratonic terranes at the ancient pacific margin of North America: Geological Association of Canada Special Paper 45, p. 25–74.

Dusel-Bacon, Cynthia, Lanphere, M.A., Sharp, W.D., Layer, P.W., and Hanson, V.L., 2002, Mesozoic thermal history and timing of structural events for the Yukon-Tanana Upland, east-central Alaska—$^{40}Ar/^{39}Ar$ data from metamorphic and plutonic rocks: Canadian Journal of Earth Sciences, v. 39, p. 1013–1051.

Dusel-Bacon, Cynthia, Wooden, J.L., and Bressler, J.R., 2001, New U-Pb zircon and geochemical evidence for bimodal mid-Paleozoic magmatism and syngenetic base metal mineralization in the Yukon-Tanana terrane, Alaska: Geological Society of America Abstracts with Programs, p. A-185.

Foster, H.L., 1992, Geologic map of the eastern Yukon-Tanana region, Alaska: U.S. Geological Survey Open-File Report 92–313, scale 1:500,000.

Foster, H.L., Albert, N.R.D., Griscom, Andrew, Hessin, T.D., Menzie, W.D., Turner, D.L., and Wilson, F.H., 1979, The Alaskan mineral resource assessment program—Background information to accompany folio of geologic and mineral resource maps of the Big Delta quadrangle, Alaska: U.S. Geological Survey Circular 783, 19 p.

Hansen, V.L., and Dusel-Bacon, Cynthia, 1998, Structural and kinematic evolution of the Yukon-Tanana Upland tectonites, east-central Alaska—A record of late Paleozoic to Mesozoic crustal assembly: Geological Society of America Bulletin, v. 110, p. 211–230.

Ludwig, K.R., 1999, User's manual for Isoplot/Ex version 2.00, a geochronological toolkit for Microsoft Excel: Berkeley, Calif., Berkeley Geochronology Center, Special Publication No. 1, 46 p.

Ludwig, K.R., 2001, Squid 1.02—A user's manual: Berkeley, Calif., Berkeley Geochronology Center, Special Publication No. 2, 21 p.

Nelson, J.L., Colpron, Maurice, Piercey, S.J., Dusel-Bacon, Cynthia, Murphy, D.C., and Roots, C.J., 2006, Paleozoic tectonic and metallogenetic evolution of pericratonic terranes in Yukon, northern British Columbia and eastern Alaska, 2006, *in* Colpron, Maurice, and Nelson, JoAnne, eds., Paleozoic evolution and metallogeny of pericratonic terranes at the ancient pacific margin of North America: Geological Association of Canada Special Paper 45, p. 323–360.

Newberry, R.J., Bundtzen, T.K., Clautice, K.H., Combellick, R.A., Douglas, Tom, Laird, G.M., Liss, S.A., Pinney, D.S., Reifenstuhl, R.R., and Solie, D.N., 1996, Preliminary geologic map of the Fairbanks mining district, Alaska: Alaska Division of Geological and Geophysical Surveys Public Data File 96-16, 17 p., 2 sheets, scale 1:63,360.

Newberry, R.J., Layer, P.W., Burleigh, R.E., and Solie, D.N., 1998, New $^{40}Ar/^{39}Ar$ dates for intrusions and mineral prospects in the eastern Yukon-Tanana terrane, Alaska—Regional patterns and significance: U.S. Geological Survey Professional Paper 1595, p. 131–159.

O'Neill, J.M., Day, W.C., Aleinikoff, J.N., and Saltus, R.W., 2005, The Black Mountain tectonic zone—A long-lived lithospheric shear zone in the Yukon-Tanana Upland of east-central Alaska: Geological Society of America Abstracts with Programs, v. 37, no. 7, p. 82.

Piercey, S.J., Nelson, J.L., Colpron, Maurice, Dusel-Bacon, Cynthia, Simard, R.L., and Roots, C.F., 2006, Paleozoic magmatism and crustal recycling along the ancient Pacific margin of North America, northern Cordillera, *in* Colpron, Maurice, and Nelson, JoAnne, eds., Paleozoic evolution and metallogeny of pericratonic terranes at the ancient pacific margin of North America: Geological Association of Canada Special Paper 45, p. 281–322.

Rombach, Cameron, 1999, Alaska resource data file—Big Delta quadrangle: U.S. Geological Survey Open-File Report 99-354, 145 p. Available at URL http://ardf.wr.usgs.gov/ardf_data/BigDelta.pdf

Saltus, R.W., 2005, Gravity and aeromagnetic gradients within the Yukon-Tanana Upland, Big Delta quadrangle east-central Alaska: Geological Society of America Abstracts with Programs, v. 37, no. 7, p. 82.

Saltus, R.W., and Day, W.C., 2006, Gravity and aeromagnetic gradients within the Yukon-Tanana Upland, Black Mountain tectonic zone, Big Delta quadrangle, east-central Alaska: U.S. Geological Survey Open-File Report 2006–1391, 1 sheet.

Saltus, R.W., and Simmons, G.C., 1997, Composite and merged aeromagnetic data for Alaska—A web site for distribution of gridded data and plot files: U.S. Geological Survey Open File Report 97–520. Available at URL http://pubs.usgs.gov/of/1997/ofr-97-0520/alaskamag.html

Selby, David, Creaser, R.A., Hart, C.J.R., Rombach, C.S., Thompson, J.F.H., Smith, M.T., Bakke, A.A., and Goldfarb, R.J., 2002, Absolute timing of sulfide and gold mineralization—A comparison of Re-Os molybdenite and Ar-Ar mica methods from the Tintina gold belt, Alaska: Geology, v. 30, no. 9, p. 791–794.

Smith, Moira, 2000, The Tintina gold belt—An emerging gold district in Alaska and Yukon, *in* Tucker, T., and Smith, M.T., eds., The Tintina gold belt—Concepts, exploration, and discoveries: British Columbia and Yukon Chamber of Mines, Cordilleran Roundup 2000, Special Volume 2, p. 1–3.

Smith, Moira, Thompson, J.F.H., Bressler, Jason, Layer, Paul, Mortensen, J.K., and Hidetoshi Takaoka, I.A., 1999, Geology of the Liese Zone, Pogo Property, east-central Alaska: Society of Economic Geologists Newsletter, no. 38, p. 1–21.

Weber, F.R., Foster, H.L., Keith, T.E.C., and Cantelow, A.L., 1975, Reconnaissance geologic map of the Big Delta A-1 and B-1 quadrangles, Alaska: U.S. Geological Survey Miscellaneous Field Studies Map MF–676, 1 plate, scale 1:63,360.

Weber, F.R., Foster, H.L., Keith, T.E.C., and Dusel-Bacon, Cynthia, 1978, Preliminary geologic map of the Big Delta quadrangle, Alaska: U.S. Geological Survey Open-File Report 78–529–A, scale 1:250,000.

Werdon, M.B., Newberry, R.J., Athey, J.E., and Szumigala, D.J., 2004, Bedrock geologic map of the Salcha River—Pogo area, Big Delta quadrangle, Alaska: Alaska Division of Geological and Geophysical Surveys Report of Investigations 2004-1b, 19 p., 1 sheet, scale 1:63,360.